HHS Public Access

Author manuscript

Biotechnol Bioeng. Author manuscript; available in PMC 2017 June 01.

Published in final edited form as:

Biotechnol Bioeng. 2016 June ; 113(6): 1357–1368. doi:10.1002/bit.25899.

Bioengineered Glaucomatous 3D Human Trabecular Meshwork as an *in vitro* Disease Model

Karen Y. Torrejon[1], **Ellen L. Papke**[1], **Justin R. Halman**[1], **Judith Stolwijk**[1], **Cula N. Dautriche**[1], **Magnus Bergkvist**[1], **John Danias**[2], **Susan T. Sharfstein**[1], and **Yubing Xie**[1,*]

[1]Colleges of Nanoscale Science and Engineering, SUNY Polytechnic Institute, 257 Fuller Road, Albany, New York, 12203, USA

[2]Department of Ophthalmology, SUNY Downstate Medical Center, 450 Clarkson Avenue, Brooklyn, New York, 11203, USA

Abstract

Intraocular pressure (IOP) is mostly regulated by aqueous humor outflow through the human trabecular meshwork (HTM) and represents the only modifiable risk factor of glaucoma. The lack of IOP-modulating therapeutics that targets HTM underscores the need of engineering HTM for understanding the outflow physiology and glaucoma pathology *in vitro*. Using a 3D HTM model that allows for regulation of outflow in response to a pharmacologic steroid, a fibrotic state has been induced resembling that of glaucomatous HTM. This disease model exhibits HTM marker expression, ECM overproduction, impaired HTM cell phagocytic activity and outflow resistance, which represent characteristics found in steroid-induced glaucoma. In particular, steroid-induced ECM alterations in the glaucomatous model can be modified by a ROCK inhibitor. Altogether, this work presents a novel *in vitro* disease model that allows for physiological and pathological studies pertaining to regulating outflow, leading to improved understanding of steroid-induced glaucoma and accelerated discovery of new therapeutic targets.

Keywords

trabecular meshwork; SU-8; 3D culture; steroid-induced glaucoma; intraocular pressure; outflow

Introduction

Glaucoma is a leading cause of blindness worldwide, affecting over 80 million people (Quigley and Broman 2006). Given the world's aging population, cases of glaucoma are expected to increase rapidly over the next ten years. There is currently no cure for this disease. The only modifiable risk factor for glaucoma is elevated intraocular pressure (IOP). In the human eye, homeostatic IOP is maintained by formation and drainage of the aqueous

*Corresponding author: Yubing Xie, Ph.D., Associate Professor, Colleges of Nanoscale Science and Engineering, SUNY Polytechnic Institute, 257 Fuller Road, Albany, NY 12203, Phone: (518) 956-7381, Fax: (518) 437-8687, YXie@sunypoly.edu.

The authors have no conflict of interest to declare.

Supporting Information: Additional supporting information may be found in the online version of this article at the publisher's web-site.

humor, primarily through the human trabecular meshwork (HTM). Approximately 70-90% of the aqueous humor is drained through this tissue (Gabelt and Kaufman 2003) and it is believed that a decrease in outflow through the TM leads to elevated IOP. Therefore, understanding the glaucoma pathology at the HTM may give rise to novel, TM-targeted therapies to treat this disease. Current research in the field is hampered by the lack of a realistic *in vitro* HTM-based model that can allow for more efficient and species-relevant pathological outflow studies and/or drug screening.

Although multiple *in vivo* animal models and *ex vivo* organ cultures, in addition to conventional 2D cell cultures, have been utilized to study effects of steroids on the TM, the field is lacking a species-relevant 3D *in vitro* model that allows for extensive studies pertaining to physiological outflow along with biological changes caused by steroids. Such a 3D *in vitro* model would further our current understanding of the pathology of steroid-induced glaucoma, and most importantly, could pave the path for the discovery of novel glaucoma targets. We have previously established an *in vitro* 3D HTM model that recapitulates the biological and physiological characteristics of HTM and behaves similarly to *ex vivo* organ cultures in response to IOP-lowering agents, e.g., latrunculin-B (Lat-B) (Torrejon et al. 2013). The ability to recapitulate pathological changes could further strengthen this model and address the need for a 3D glaucomatous HTM for biological and outflow studies, as well as drug screening.

The administration of steroids, such as corticosteroids, used to treat inflammation either topically or systematically, has long been linked to primary open-angle glaucoma (POAG) (Behbehani et al. 2005; Bernstein et al. 1963; Cubey 1976; Garbe et al. 1997; Garrott and Walland 2004; Kalina 1969). In susceptible patients, steroids can lead to the development of ocular hypertension and POAG (Becker and Mills 1963; Bernstein et al. 1963; Jones and Rhee 2006; Kersey and Broadway 2006). If left untreated, these conditions can cause glaucomatous optic neuropathy, in turn leading to irreversible vision loss. Steroid-induced glaucoma is associated with morphological and biological changes in the HTM *in vivo*, which in turn, are believed to reduce aqueous humor outflow (Bernstein and Schwartz 1962). The morphological and physiological changes induced by steroids in the HTM bear a resemblance to those seen in the pathogenesis of POAG. Among the most studied changes are (a) increased extracellular matrix (ECM) deposition in the juxtacanalicular tissue (cribriform region) (Ueda et al. 2002), (b) decreased intra-trabecular spaces (Fautsch et al. 2000), (c) myocilin protein induction, (d) cytoskeletal element rearrangement (Clark et al. 2005; Hoare et al. 2009; Read et al. 2007; Tripathi et al. 1989), (e) inhibition of phagocytosis (Matsumoto and Johnson 1997a; Matsumoto and Johnson 1997b) and (f) increased outflow resistance. Since the HTM accounts most of aqueous humor outflow in the eye (Tripathi and Tripathi 1989), changes in this tissue could have detrimental effects on IOP homeostasis. Rho-associated kinase (ROCK) inhibitors have demonstrated reduction of IOP in several animal models by increasing aqueous humor drainage through the trabecular meshwork (TM) due to disruption of actin fibers (Tian and Kaufman 2005; Tokushige et al. 2007). Several ROCK inhibitors are currently undergoing clinical trials as a potential new class of glaucoma drugs (Tanihara et al. 2008; Tanihara et al. 2013; Williams et al. 2011). However, using ROCK inhibitors in combination with steroid-based anti-inflammatory agents to lower IOP is yet to be explored.

Here we demonstrate that the bioengineered 3D HTM model recapitulates glaucoma characteristics *in vitro,* similar to those seen in susceptible humans treated with steroids. Further characterization of bioengineered glaucomatous 3D HTM constructs, shows induction of myocilin, ECM deposition, rearrangement of cell cytoskeleton, impaired phagocytosis, elevated outflow resistance and reduced outflow facility; demonstrating the utility of our model as a powerful tool to help understand disease mechanisms by which extended steroid treatment induces glaucomatous HTM and hence, increases IOP. Furthermore, we investigated its applicability to test anti-glaucoma agents using the ROCK inhibitor as a model agent.

Materials and Methods

Primary Human Trabecular Meshwork Cell Culture

HTM cells were isolated from donor tissue rings discarded after penetrating keratoplasty. Isolation of the cells was performed under an IRB exempt protocol approved by the SUNY Downstate IRB. Isolation and culture conditions were as previously described (Torrejon et al. 2013) . Before use in experiments, all HTM cell strains were characterized for expression of αB-crystallin and α-smooth muscle actin. HTM cells were initially plated in 75 cm^2 cell culture flasks with 10% fetal bovine serum (FBS) (Atlas Biologicals, Fort Collins, CO) in Improved MEM (IMEM) (Corning Cellgro, Manassas, VA) with 0.1 mg/mL gentamicin. Fresh medium was supplied every 48 h. Cells were maintained at 37 °C in a humidified atmosphere with 5% carbon dioxide until 80-90% confluence, at which point cells were trypsinized using 0.25% trypsin/0.5 mM EDTA (Gibco, Grand Island, NY) and subcultured. At least three donors' human primary cell cultures were used during experiments. All studies were conducted using cells before the 5^{th} passage.

Biomimetic Scaffold Fabrication

SU-8 2010 (MicroChem Corp.) was used to develop free-standing biomimetic porous microstructures that served as scaffolds on which primary HTM cells were cultured. Scaffolds were fabricated using standard photolithographic techniques as previously described (Torrejon et al. 2013). Briefly; a release layer was spin-coated on the wafer and baked at 150 °C. SU-8 2010 was applied by spin-coating to final thickness of 5 μm, then baked at 95 °C and cooled to room temperature. The resist was UV-exposed through a mask containing the desired pattern, baked at 95°C and developed in PGMEA developer (MicroChem Corp.) SU-8 scaffolds with the desired features were released from the substrate, washed with acetone and sterilized using 70% ethanol.

3D Culture of HTM Cells on Scaffolds and Prednisolone Acetate (PA) Treatment

To create 3D HTM constructs, 40,000 HTM cells were seeded on each SU-8 scaffold placed in a 24-well plate and cultured in 10% FBS-IMEM for 14 days. Medium was changed every 2-3 days. On day 14, 3D HTM constructs were serum-starved for 48 hrs and then treated with PA (Sigma Aldrich, ST. Louis, MO) (3, 30, 300, 3000 and 30000 nM) or vehicle alone (0.1% ethanol) for 3, 6, or 9 days, as indicated. Out of the four donors' HTM cells being used, three were PA-responsive while one did not appear to be affected by PA. Hence three PA-responsive HTM cell strains were used for the remaining studies. After comparing the

effect of PA concentration on selected protein expression, in all subsequent experiments, 3D HTM cultures on the scaffolds were treated with 300 nM PA, vehicle (ethanol), 10 μM Y27632, or 300 nM PA/10 μM Y27632 (Sigma Aldrich).

Protein Extraction and Western Blot Analysis

To quantify secreted protein expression, medium samples were collected on days 3, 6 and 9 and concentrated 4× with centrifugal ultrafiltration columns (Centricon YM-10; Millipore, Bedford MA). Cellular proteins were extracted with radioimmunoprecipitation assay (RIPA) buffer containing protease inhibitors (Complete Protease Inhibitor, Roche, Manheim, Germany) on ice. Proteins were quantified by bicinchoninic acid assay (Thermo Fischer Scientific). 25 μg of proteins from each sample were separated by SDS polyacrylamide gel electrophoresis on a 4-12% gel in MOPS running buffer (Life Technologies), transferred onto PVDF membrane and probed with primary antibodies against myocilin(Sigma Aldrich), fibronectin, collagen IV, αβ-crystallin and β-actin (Abcam), followed by incubation with HRP-conjugated secondary antibodies (Invitrogen) and detection using FluorChem E (Protein Simple). Protein expression was analyzed by densitometry using ImageJ, and normalized to house keeping β-actin. All experiments were performed in triplicate for each of three donor cell.

Immunocytochemistry Followed by Confocal Microscopy

After 14 days in culture, 3D HTM constructs were serum-starved in 1% FBS and treated with 300 nM PA, 300nM PA/10 μM Y27632, or vehicle alone for 9 days. 3D HTM samples were fixed, permeablized, and incubated with antibodies against HTM markers myocilin, and αB-crystallin, and ECM proteins, collagen type IV, fibronectin and laminin (Abcam), as described previously (Torrejon et al. 2013). Followed by incubation with appropriate secondary antibodies. Laser scanning confocal microscopy was performed using a Leica SP5 confocal microscope, and images were acquired at 40× and 63× magnifications with an oil-immersion objective using the same laser intensity and gain settings in order to be able to compare intensities across samples.

Cytoskeletal Staining and Nuclear Size Analysis

3D HTM samples were fixed and stained for F-actin cytoskeleton using phalloidin (Life Technology) and co-stained with DAPI to reveal cell nuclei, followed by confocal imaging. Nuclei size measurements were done using ImageJ. Fifteen images from seven control samples and twenty images from eight PA-treated samples were used for nuclear size analysis.

Scanning Electron Microscopy

3D HTM samples were fixed, dehydrated and sputter-coated to prevent charging. Samples were observed under a LEO 1550 field emission scanning electron microscope (SEM) (Leo Electron Microscopy Ltd, Cambridge, UK) as described previously (Torrejon et al. 2013).

Phagocytosis Assay—Cultures of 3D HTM were challenged with *E. coli* conjugated to pHrodo green particle dyes (0.5 mg/well, Life Technologies) and incubated for 3 hours.

These bioparticle conjugates are non-fluorescent outside the cell, but fluorescent at acidic pH in phagosomes. After the incubation, nuclei were stained with NucBlue live cell stain (Life Technologies) and cultures were imaged using fluorescence microscopy. Fluorescence was quantified using a live-cell multi-plate reader (Tecan, Männedorf, Switzeland). All experiments were performed in triplicate using three donor cell strains.

Electric-Cell-Substrate Impedance Sensing

To measure the transcellular electrical resistance across 3D HTM constructs, Electric Cell-Substrate Impedance Sensing (ECIS®) (Giaever and Keese 1984; Stolwijk et al. 2014) (Applied Biophysics Inc., Troy, NY) was used. The SU-8 scaffolds on 6.5 mm filter inserts were inserted into an ECIS Trans-Filter Adapter for parallel measurement of up to 8 filters at a time and measured using an ECIS Zθ (Theta) instrument. A non-invasive alternating current was applied and the complex impedance across the SU-8 scaffold between the bottom and top electrode was measured. Resistance was monitored at a frequency of 1000 Hz with a temporal resolution of 22 data points per hour. The frequency of 1000 Hz was selected for monitoring as previous study of cell-covered and cell-free scaffolds showed a maximum resistance ratio at this particular frequency (Figure S1). Before starting measurement and after every medium change, SU-8 scaffolds were microscopically inspected for any possible defects. Resistance of a cell-free filter in medium was about 100 Ω at 1000 Hz. HTM cells were cultured for 14 days on the scaffolds to create 3D HTM constructs before resistance was recorded (denoted as day 0). Medium was exchanged every 2 – 3 days, adding 300 nM fresh PA to the treated samples each time. On day 11 of PA treatment, 3D HTM constructs were treated with 10 μM Lat–B in order to reverse the effect of PA. Untreated samples were used as the controls. Experiments were run in quadruplicate, using three donors' cells.

Perfusion Studies

A perfusion apparatus was used as previously described (Torrejon et al. 2013). After at least 7 days of PA treatment, samples were securely placed in the perfusion chamber and perfused at various rates for 6 hrs per flow rate (2, 10, 20 and 40 μl/min). Samples were perfused in an apical-to-basal direction with perfusion medium consisting of Dulbecco's modified Eagle's medium (DMEM) (Cellgro) with 0.1% gentamicin (MP) containing 300 nM PA. The temperature was maintained at 34 °C, which simulates the temperature of the cornea of the eye and widely used for *ex vivo* perfusion studies of TM. Pressure was continuously monitored and recorded. After perfusion, samples were fixed and stained for SEM or confocal imaging. The “outflow facility” of our bioengineered 3D HTM model, Δflow/Δpressure, was calculated from the inverse of the slope of the pressure versus flow graph per unit surface area. Twelve different samples per condition including HTM cells from three donors were studied under perfusion.

Normalization of the Outflow Facility to Surface Area

By taking into account the circumference of a human eye (assuming an eye of 12 mm in diameter) with a TM of 100 μm in width, the surface area of filtering HTM (π × 12 mm × 0.10 mm) is ∼3.8 mm^2. *In vivo* outflow facility of normal human eye is 0.3-0.4 μL/min/mmHg, and therefore, in terms of outflow facility per unit area, it translated to 0.078-0.106

$\mu L^{-1}min^{-1}mmHg^{-1}mm^2$. The outflow facility per unit area ($\mu L^{-1}min^{-1}mmHg^{-1}mm^2$) of our bioengineered 3D HTM will be calculated based on the surface area of the 3D HTM construct as well.

Quantitative Real-time PCR (qPCR) Analysis

Total RNA was extracted from samples cultured for 3, 5, and 9 days with or without PA treatment using an RNeasy Plus Mini kit (Qiagen Inc., Valencia, CA). RNA concentrations were determined using a NanoDrop spectrophotometer (Thermo Scientific, Wilmington, DE). qPCR was carried out using TaqMan RNA-to-CT™ 1-Step Kit (Applied Biosystems, Carlsbad, CA) and performed on an AB StepOnePlus Real Time PCR system (Life Technologies, Carlsbad, CA) using primers for MMP2, MMP3, IL-1α, TIMP-1 and TGFβ (Table S1).The temperature profile was as follows: 48°C for 15 min (reverse transcription step), followed by an enzyme activation step of 95°C for 10 min, 40 cycles of 15 s denaturation at 95°C and 1 min anneal/extend at 60°C. Relative quantitation data analysis was performed using the comparative quantification method, ΔΔCt, with GAPDH as the endogenous reference. All samples were normalized to the vehicle-treated controls. qPCR experiments were performed in triplicate from duplicate biological experiments using three donor cells. Average values are presented as mean ± SD.

Statistical Analysis

Data were expressed as the average ± standard deviation. Student's t-test was performed for nuclear size analysis and phagocytosis assay. The difference between controls, PA-treated, and PA/ Y27632-treated 3D HTM samples was analyzed using two-way ANOVA followed by Bonferroni post-tests (GraphPad Prism 6.02; GraphPad Software, Inc., La Jolla, CA). $P < 0.05$ and $P < 0.001$ considered significant and highly significant, respectively.

Results

Creation and Characterization of Glaucomatous 3D Human Trabecular Meshwork Model

To engineer an *in vitro* HTM model that recapitulates the pathology of steroid-induced glaucoma, photolithographic techniques in combination with 3D cell culture of primary HTM cells, followed by extended steroid treatment was employed (Scheme 1). Prednisolone acetate (PA), which is a frequently used ophthalmic (anti-inflammatory) corticosteroid drug, was used as a model steroid. The micropatterned, well-defined, porous SU-8 scaffold was first fabricated using photolithography, which has the pore size of 12 μm, beam width (spacing between two neighboring pores) of 7 μm and thickness around 5 μm. It has shown to support growth and proliferation of primary HTM cells in an architecture that mimics the biochemical and outflow environment of the HTM *in vivo* (Torrejon et al. 2013). Primary HTM cells were seeded on gelatin-coated SU-8 scaffolds and cultured for 14 days as described previously, forming 3D HTM layers of 40-μm thickness (Torrejon et al. 2013). We next examined the effects of PA concentrations (3 nM to 30 μM) on HTM marker expression for over 9-day treatment without perfusion. We observed induced myocilin and increased ECM proteins of fibronectin and collagen IV, characteristics seen in patients with steroid-induced glaucoma. A significant maximum response was observed at a concentration of 300 nM PA for both intracellular and secreted myocilin and fibronectin as well as secreted

collagen IV (Figure 1A-B). Therefore, we used 300 nM PA to treat 3D HTM to induce glaucomatous state for the remainder of these studies.

Changes in myocilin and ECM protein expression after PA perfusion were confirmed by immunocytochemistry analysis, revealing rearranged patterns of these secreted proteins. After PA perfusion for 9 days, secreted myocilin appeared amorphous and plaque-like, while collagen IV and fibronectin seemed remodeled into densely packed, thin fibrous arrangements (Figure 1C). In multiple PA-treated samples from multiple donor HTM cells, we consistently observed nodular, aggregated vertices formed by secreted collagen IV fibers, with a greater level of collagen IV expression than untreated cultures (Figure 1C, middle panel). The fine fibrils of collagen IV and fibronectin appeared denser and more organized than those in control cultures, similar to those described in human eyes with corticosteroid-induced glaucoma (Johnson et al. 1997). Altogether, the induction of myocilin expression and increase in ECM deposition after PA treatment suggests that the bioengineered 3D HTM is responsive to steroids and induced to a glaucomatous state.

Given the increased attention to cytoskeletal rearrangements that have been described in patients with glaucomatous HTM, we examined whether similar changes were induced by PA perfusion in our model. Phalloidin-stained F-actin in HTM cells showed increased actin fibers after exposure to 300 nM PA for 9 days, several of which joined together into bundles, demonstrating crosslinked actin networks (CLANs) (Figure 2A-C). The CLANs observed in the 3D HTM were similar in architecture to those reported after dexamethasone (DEX) treatment in organ culture models as well as histological samples of glaucomatous HTM (Hoare et al. 2009; Johnson et al. 1997; Read et al. 2007). Moreover, cells treated with PA in 3D HTM had significantly larger nuclei compared to vehicle controls (Figure 2D). Enlarged nuclei have previously been reported in DEX-induced glaucoma *ex vivo* (Clark et al. 1995) and are associated with activated HTM cells. Scanning electron microscopy (SEM) revealed differences in the surface topography with larger amounts of amorphous fibrillary material in the PA-treated cultures. HTM cells appeared embedded and even covered by this material, reducing intercellular spacing (Figure 2E-F). Furthermore, compared to vehicle-perfused controls where the cell surface was fairly smooth and cells were easily distinguished (Figure 2E), in PA-perfused samples, the cell surface appeared rough and surrounded by plaque material (Figure 2F).

Functional Properties of the Glaucomatous 3D Human Trabecular Meshwork

Functional properties of HTM cells were further analyzed to assess whether these steroid-induced glaucomatous morphological changes enhanced or impaired cellular functions. The phagocytic activity of 3D HTM was assessed using *E. coli* labelled with pH-sensitive dye. After treatment with 300 nM PA, only 5-10% of the PA-treated HTM cells were phagocytic, compared with 20-30% of HTM cells in vehicle-treated controls (Figure 3A-B), demonstrating a statistically significant decrease in phagocytic activity (Figure 3C), similar to that reported after DEX treatment *in situ* (Matsumoto and Johnson 1997a).

We further characterized the pressure-independent transcellular electrical resistance towards ionic species in the medium of the 3D HTM using real-time monitoring of electric cell-substrate impedance sensing (ECIS) (Giaever and Keese 1984). The impedance was

recorded before treatment, where no significant difference was observed between 3D HTM samples. Subsequently, samples were either treated with 300 nM PA or vehicle alone (control) for 11 days, throughout which impedance was continuously monitored (Figure 4A). Medium was changed every two to three days, causing a spike in the impedance curve. Increased impedance was observed over time in PA-treated cultures compared to the vehicle-treated controls and, in particular, during days 9 through 11, establishing greater electrical resistance differences. To analyze the effect of actin networks on the increased transcellular electrical resistance caused by PA treatment, PA-treated 3D HTM was challenged with the actin disruptor Lat-B, an IOP-lowering agent, on day 11 for 3 hours while the resistance was continuously recorded. Lat-B rapidly decreased the electrical resistance across these samples, stabilizing after 3 hours. Even after Lat-B action, the resistance of the PA-treated constructs was still significantly higher (125 ± 2.3 Ω) than vehicle controls (110 ± 2.6 Ω) ($P < 0.001$) (Figure 4B), suggesting changes resulting from PA treatment beyond actin rearrangements.

One of the main functions of the HTM is to regulate aqueous humor outflow. Under glaucomatous condition, transcelluar pressure increases, and therefore, the outflow facility decreases. To examine the ability of our 3D HTM model to regulate outflow in response to steroid, we utilized a perfusion apparatus (Torrejon et al. 2013) to study the hydrodynamic behavior, in which the rate of perfusate flow was controlled while recording the transmembrane pressure across the 3D HTM (Figure 4C). Compared to vehicle controls, PA perfusion significantly decreased the outflow facility across the 3D HTM (Figure 4D). Control cultures showed an outflow facility of 0.131 ± 0.003 $\mu L^{-1}min^{-1}mmHg^{-1}mm^2$ while PA treatment significantly lowered the outflow facility of the bioengineered 3D HTM to 0.093 ± 0.004 $\mu L^{-1}min^{-1}mmHg^{-1}mm^2$. These data demonstrate that the bioengineered 3D HTM is steroid-responsive, regulating perfusate flow in a similar fashion as aqueous humor outflow regulation seen in *in vivo* and *ex vivo* glaucomatous HTM, by increasing pressure and decreasing the outflow facility across this tissue.

Response of the Steroid-induced Glaucomatous 3D HTM Model to ROCK Inhibitor

To explore the use of ROCK inhibitors to arrest the drastic effects induced by PA treatment on the HTM ECM remodeling, we treated 3D HTM with a combination of these two agents: 300 nM PA and/or 10 μM Y27632, a ROCK inhibitor. Compared to PA alone, the presence of ROCK inhibitor during PA treatment caused no significant change in myocilin expression, but significantly decreased ECM proteins, including collagen IV and fibronectin ($N=9$, $P < 0.001$ for both proteins) (Figure 5A-B). These trends were confirmed by immunocytochemistry (Figure 5C) and qPCR analysis (Figure 5D). Compared to vehicle controls, cells co-treated with PA and Y27632 still exhibited significantly higher expression of intracellular myocilin ($P < 0.05$) and αB-crystallin ($P < 0.01$), but lower fibronectin expression ($P < 0.05$) (Figure 5A-B). Compared to controls, Y27632 alone elevated myocilin expression ($P < 0.001$) at both protein (Figure 5B) and mRNA level (Figure 5D). Compared to PA treatment, Y27632 alone significantly decreased expression of collagen IV and fibronectin at both protein (Figure 5B) and mRNA level (Figure 5D).

Given the observed changes in ECM protein deposition, we evaluated gene expression of matrix metalloproteinase (MMP)-2 and -3 with PA and/or Y27631 treatment for 9 days, which are enzymes responsible for degradation and remodeling of the ECM at the conventional outflow pathway. Imbalances in the expression of these MMPs have been linked to POAG and corticosteroid treatments (De Groef et al. 2013; Pang et al. 2003; Snyder et al. 1993). Similarly, increased MMP expression has been described soon after mechanical or pressure-induced homeostatic response in organ cultures of the anterior eye segment (Vittitow and Borras 2004). MMP-2 gene expression significantly increased ∼2.4-fold after a 3-day PA-treatment compared to vehicle controls (Figure 6A). This increase was eliminated by PA/Y27631 co-treatment. However, after 5-day treatment, neither showed any difference from control cultures. Interestingly, MMP-2 gene expression significantly decreased ∼1.8-fold after 9-day PA treatment and to a greater extent (∼2.2-fold, $P < 0.001$) with PA/Y27632 treatment (Figure 6A). MMP-3 gene expression showed significant decrease between control, PA (∼ 4-fold, $P < 0.001$), and PA/Y27632 (∼1.7-fold, $P < 0.001$) treatment at day 3 and day 5 (∼7-fold, $P < 0.01$ and ∼3.7-fold, $P < 0.001$; respectively). By day 9, MMP-3 expression was down-regulated to a greater extend, ∼150-fold ($P < 0.001$) for PA treatment and 49-fold ($P < 0.001$) for PA/Y27632 treatment, respectively (Figure 6B).

HTM cells secrete several cytokines that modulate cell behavior and ECM turnover in the conventional outflow pathway. Therefore, we investigated whether the transcriptional expression of these cytokines was modulated as a result of PA treatment, which could provide insight into the pathology of steroid-induced glaucoma. Increased cytokine expression has been observed in the aqueous humor of glaucoma patients, including tissue inhibitor of metalloproteinase-1 (TIMP-1) (Gonzalez-Avila et al. 1995) and transforming growth factor-β (TGFβ) (Tripathi et al. 2004; Tripathi et al. 1994). In addition, interleukin 1-alpha (IL-1α) is an inflammatory cytokine that can regulate outflow facility (Bradley et al. 1998). Transcriptional expression of cytokines IL-1α, TIMP-1 and TGFβ was studied in response to PA alone and PA/Y27632 treatment. IL-1α mRNA expression was down-regulated 21-fold, 41-fold, and 16-fold ($P < 0.001$ for each) after PA treatment for 3, 5 and 9 days, respectively (Figure 7A). Treatment with Y27632 ROCK inhibitor exhibited a time-dependent effect on IL-1α mRNA expression during PA treatment. On days 3 and 5 after initiation of PA/Y27632 treatment, the PA-induced decrease in IL-1α gene expression was partially relieved by the presence of Y27632, but still 10-($P < 0.05$) and 17-fold ($P < 0.05$) lower than untreated controls, respectively. On day 9, the presence of Y27632 during PA treatment caused an even greater decrease in IL-1α gene expression (61-fold) compared to untreated controls ($P < 0.001$). While TIMP-1 mRNA expression was up-regulated 4- ($P < 0.001$) and 2-fold ($P < 0.05$) after 3 and 5 days of PA-treatment, it was down-regulated 2-fold ($P < 0.001$) after day 9 (Figure 7B). On the other hand, co-treatment with Y27632 during PA treatment obviated changes in TIMP-1 gene expression for all 9 days. TGFβ gene expression was down-regulated on days 3 and 5 by PA treatment (1.2- and 3.2-fold) and to a greater extent during PA/Y27632 co-treatment (4.8- and 2.8, $P < 0.001$ for all) (Figure 7C). Despite its initial down-regulation, TGFβ gene expression was up-regulated over 3.7-fold by PA treatment for 9 days suggesting potential bi-phasic response. Given TGFβ's ability to enhance ECM protein expression and deposition that can block paracellular pores in the HTM, this final increased expression of TGFβ in PA-treated 3D HTM could account for the

greater suppression of MMPs observed on day 9 and increased transcellular electrical resistance seen at the same time. Although extended analysis of steroid effects on TGFβ expressed by TM cells has not been reported previously, studies performed using human lung fibroblast cells have shown that steroid modulates TGFβ production (Wen et al. 2003), and similar to these studies, several days of PA treatment initially inhibited TGFβ. The presence of Y27632 during PA treatment reduced TGFβ gene expression back to the control level on day 9. This is the first time, to our knowledge, that effects of extended treatment with PA in the presence and absence of ROCK inhibitors on gene expression of these cytokines have been examined. The dynamic pattern of MMP and cytokine gene expression also highlights the importance of a 3D HTM model that is suitable for long-term drug treatment studies.

Discussion

The density and deposition of ECM proteins in our bioengineered, steroid-induced glaucomatous 3D HTM model was significantly greater than that in normal HTM controls. Steroid-induced elevation of IOP is generally believed to be caused by increased resistance to aqueous outflow through associated changes in the TM and its ECM (Clark et al. 1995; Johnson et al. 1997; Johnson et al. 1990; Yue 1996). Increased expression of ECM proteins has been reported in humans after exposure to corticosteroids (Johnson et al. 1990). In our 3D HTM model, we qualitatively and quantitatively evaluated the increased expression of fibronectin and collagen IV proteins after corticosteroid treatment, which is consistent with organ perfusion models (Samples et al. 1993; Zhou et al. 1998). Furthermore, myocilin was also expressed and elevated in our model, which reflects the *in vivo* glaucomatous HTM. Densitometry analysis of intracellular and secreted myocilin and fibronectin as well as secreted collagen IV, showed a biphasic dose-response to PA. The immunocytochemistry of the secreted collagen IV and fibronectin revealed different topographical/morphological patterns between the PA-treated samples and vehicle controls. Both proteins exhibited greater amounts of ECM-crosslinked fibers, suggesting increased matrix assembly, which may be in part responsible for the increased resistance across this tissue.

ECM turnover is tightly regulated by balancing assembly and degradation through MMPs, TIMPs and structural proteins. MMPs are secreted by HTM cells and are responsible for breaking down ECM proteins and remodeling the ECM (De Groef et al. 2013). MMP-2 and -3 are thought to help maintain homeostasis of the conventional outflow architecture (Conley et al. 2004; Tripathi et al. 2004). MMP-2 and MMP-3 both degrade gelatin, collagen IV and fibronectin. Several studies demonstrated that agents to modulate outflow facility in perfusion cultures can affect the expression/activation of these MMPs (Bahler et al. 2008; Sanka et al. 2007). Therefore, the decreased MMP-2 and -3 gene expression, particularly after extended PA treatment could account for the increased amounts of ECM observed. Initial MMP-2 increases suggest that in steroid-induced glaucoma, TM cells strive to correct any overproduction of ECM. However, the persistent action of this MMP likely causes overproduction of replacement ECM and/or cleavage of ECM components which might not be readily accessible for degradation. With extended exposure to PA, these MMPs are down-regulated, which can leave substantial accumulated paracellular ECM at the HTM and its basement membrane as observed in this study. Likewise, phagocytosis has been proposed to

be involved in ECM turnover (Acott 1994; Matsumoto and Johnson 1997a; Zhang et al. 2007). Therefore, the decreased phagocytic activity after steroid treatment observed could create irregularities in the clearance mechanisms of HTM cells and affect ECM turnover. These irregularities might account for some of the amorphous, plaque-like material formed after PA treatment.

Steroids exert physiological effects through their interaction with cytoplasmic receptors, followed by DNA-binding and transcriptional modulation (Wordinger and Clark 1999). HTM cells contain glucocorticoid receptors, and therefore, should be steroid responsive. Steroids can induce increased cytoplasmic and nuclear areas (Tripathi et al. 1989). Our studies suggest similar actions by PA in HTM cells, which exhibited enlarged nuclei and cytoplasm. The size and shape of a nucleus depends on the interaction with the cytoskeleton and nuclear lamina. We speculate that PA-induced cytoskeletal remodeling and together with cellular activation could cause expansion of nuclear surface area, allowing nuclei to grow in size. In some instances, HTM cells lying within the fibrillary material appeared to be transformed into myofibroblasts, with prominent cytoplasmic filaments resembling actin and dense regions of the cell membrane. PA can also cause variations in transcriptional expression of cytokines. IL-1α, known to induce MMP-3 production, was down-regulated as expected, given PA's anti-inflammatory nature and association with decreased MMP-3 gene expression. Interestingly, TIMP-1 was initially up-regulated but down-regulated over time, which may inhibit the activity of certain MMPs over the initial stages of steroid exposure. TIMP-1 is a strong cytokine inhibitor of MMP-1 (Olson et al. 1997) that has been described as a potential key cytokine in ECM turnover in the conventional outflow pathway (Conley et al. 2004). Based on our results, TIMP-1 could be inhibiting the initial production of certain MMPs in an attempt to restore homeostasis but over time might be subsequently decreased, given the decrease in MMP expression/activity. The synergetic decrease of MMP-2 and TIMP-1 observed here, has been reported in previous studies focused on exogenous selenium treatments on HTM cells (Conley et al. 2004). Another cytokine that has received increased interest for its relationship with glaucoma is TGFβ. TGFβ alters ECM metabolism by suppressing MMP-3 and in turn, increases the deposition of fibronectin (Tripathi et al. 2004; Tripathi et al. 1994). TGFβ is over-expressed in glaucomatous aqueous humor and is up-regulated in corticosteroid-induced animal models (Gerometta et al. 2010). Our glaucomatous 3D HTM model demonstrated that the increase in gene expression of TGFβ is a process that may take over a week, underlying the importance of extended time-course studies when attempting to understand the transcriptional effects of corticosteroids on endogenously secreted cytokines.

The actin cytoskeleton is physically linked to the ECM through focal adhesions (Geiger et al. 2001). Contraction or disruption of the actin cytoskeleton diminished the number of adhesions between cells and ECM in several cell types (Cukierman et al. 2001; Provenzano et al. 2009). Rearrangements of the cytoskeleton of HTM cells may be affected by exposure to steroids. Steroids reorganize and remodel the TM cytoskeleton into CLANs in human anterior segments (Clark et al. 2005). To this end, several agents have been used in different fields to study the effect of cytoskeleton modulation, including cytochalasin, latrunculins, H-7, and ROCK inhibitors. Many of these agents decrease outflow resistance through cytoskeletal reorganization of the actomyosin system (the complex of actin and myosin)

when applied to the HTM (Honjo et al. 2001; Johnson 1997; Sabanay et al. 2004). Based on our ECIS studies, cytoskeletal arrangements substantially contribute to the increased transcellular electrical resistance across the 3D HTM tissue, which was shown by a dramatic decrease in impedance after Lat-B treatment. Although challenging PA-treated 3D HTM with the IOP-lowering agent, Lat-B, reduced the impedance, the final transcellular electrical resistance was still greater than that of vehicle controls. It suggests that cytoskeleton disruption alone is not sufficient to reduce the PA-induced outflow resistance to normal. The ECIS is extremely sensitive to changes in cell morphology, which are evoked by alterations in architecture of structural components including cell-cell and cell-ECM junctions (Stolwijk et al. 2014). ECM accumulation on the tissue likely affected the outflow resistance, resulting in the residual increased transcellular electrical resistance after Lat-B treatment.

Actin cytoskeleton and fibronectin matrix assembly is promoted by RhoA with contributions from ROCK I and II (Yoneda et al. 2007; Zhong et al. 1998). ROCK inhibitors are currently being studied as potential therapeutics for glaucoma management. Recent studies have demonstrated their efficacy in reducing IOP in human eyes (Kopczynski and Epstein 2014; Tanihara et al. 2008; Williams et al. 2011) through alteration of the HTM cytoskeletal arrangement and cell shape (Honjo et al. 2001; Rao et al. 2001). Here, the ROCK inhibitor, Y27632, alleviated the PA-induced increase in fibronectin and collagen IV protein and gene expression (Figure 5), which alludes to cell-ECM disruption and ECM regulations in the HTM by ROCK I and II. Co-treatment with Y27632 restored collagen IV protein expression to normal levels compared with PA treatment alone, similar to a recent *ex vivo* study in which DEX treatment significantly increased collagen IV and fibronectin gene expression while combining DEX/Y27632 mitigated the increase (Fujimoto et al. 2012). In particular, the DEX-induced decrease in outflow facility was restored to normal levels by the combined DEX/Y27632 treatment in porcine anterior segment organ cultures (Fujimoto et al. 2012). These studies suggested the involvement of the ROCK signaling pathway in corticosteroid-induced ocular hypertension. Additionally, the presence of Y27632 during PA treatment for 9 days reduced PA-induced alterations in gene expression of cytokines (e.g., TIMP-1, TGFβ) to the normal levels of 3D HTM without any other treatment.

Interestingly, expression of myocilin and αB-crystallin in PA-treated 3D HTM remained higher than controls in the presence of ROCK inhibitor. Treatment with Y27632 alone also increased myocilin, suggesting the relationship between ROCK inhibition and myocilin upregulation is complicated, which requires further investigation especially given myocilin has long been linked to glaucoma. Additionally, αB-crystallin, an understudied protein due to its lack of expression in conventional 2D cultures, is found at elevated levels in aqueous humor of POAG patients (Lutjen-Drecoll et al. 1998). Our 3D HTM model exhibits αB-crystallin expression which is increased after PA treatment. The presence of Y27632 during PA treatment does not alleviate PA-induced increase of αB-crystallin, suggesting the feasibility of studying the role of αB-crystallin in HTM physiology and pathology using our 3D HTM model.

Conclusion

We demonstrate that the bioengineered 3D HTM is responsive to PA and exhibits morphological and physiological changes, similar to glaucomatous HTM observed *in vivo* and *ex vivo*. We further validate the glaucomatous 3D HTM model and its responsiveness to an IOP-reducing agent, ROCK inhibitor Y27632. Our studies strengthen the notion that there are several factors that, together, orchestrate the increase in outflow resistance/decrease of outflow facility at the HTM to mimic steroid-induced glaucoma, including increased myocilin expression and secretion, enhanced ECM deposition, intensified actin fiber crosslinking, decreased gene expression of MMPs, increased gene expression of TGFβ, decreased phagocytosis, increased transmembrane resistance, and therefore, decreased outflow facility after 9-day PA treatment. Furthermore, these steroid-induced ECM alterations and cytokine expression in HTM can be modified by co-treatment with ROCK inhibitors. Overall, we have demonstrated a bioengineered, steroid-induced glaucomatous 3D HTM perfusion model system as clinically and physiologically relevant platform for long-term study of the physiopathology of human outflow pathway and drug testing.

Supplementary Material

Refer to Web version on PubMed Central for supplementary material.

Acknowledgments

This work is partially supported by the College of Nanoscale Science and Engineering Startup Funds (Sharfstein), NIH Grant R01 EY20670 (Danias), American Glaucoma Society Mid-Career award (Danias), SUNY Health Network of Excellence (Xie), SUNY TAF, and NSF STTR 1448900. Torrejon was supported by a National Science Foundation Graduate Research Fellowship. The authors thank Dr. Sandeep Kumar for technical support.

References

Acott, TS. Biochemistry of aqueous humor outflow. Kaufman, PL.; Mitaq, TQ., editors. Lonson: Mosby; 1994.

Bahler CK, Howell KG, Hann CR, Fautsch MP, Johnson DH. Prostaglandins increase trabecular meshwork outflow facility in cultured human anterior segments. Am J Ophthalmol. 2008; 145(1): 114–9. [PubMed: 17988642]

Becker B, Mills DW. Corticosteroids and intraocular pressure. Arch Ophthalmol. 1963; 70:500–7. [PubMed: 14078872]

Behbehani AH, Owayed AF, Hijazi ZM, Eslah EA, Al-Jazzaf AM. Cataract and ocular hypertension in children on inhaled corticosteroid therapy. J Pediatr Ophthalmol Strabismus. 2005; 42(1):23–7. [PubMed: 15724895]

Bernstein HN, Mills DW, Becker B. Steroid-induced elevation of intraocular pressure. Arch Ophthalmol. 1963; 70:15–8. [PubMed: 13967695]

Bernstein HN, Schwartz B. Effects of long-term systemic steroids on ocular pressure and tonographic values. Arch Ophthalmol. 1962; 68:742–53. [PubMed: 13967694]

Bradley JM, Vranka J, Colvis CM, Conger DM, Alexander JP, Fisk AS, Samples JR, Acott TS. Effect of matrix metalloproteinases activity on outflow in perfused human organ culture. Invest Ophthalmol Vis Sci. 1998; 39(13):2649–58. [PubMed: 9856774]

Clark AF, Brotchie D, Read AT, Hellberg P, English-Wright S, Pang IH, Ethier CR, Grierson I. Dexamethasone alters F-actin architecture and promotes cross-linked actin network formation in human trabecular meshwork tissue. Cell Motil Cytoskeleton. 2005; 60(2):83–95. [PubMed: 15593281]

Clark AF, Wilson K, de Kater AW, Allingham RR, McCartney MD. Dexamethasone-induced ocular hypertension in perfusion-cultured human eyes. Invest Ophthalmol Vis Sci. 1995; 36(2):478–89. [PubMed: 7843916]

Conley SM, Bruhn RL, Morgan PV, Stamer WD. Selenium's effects on MMP-2 and TIMP-1 secretion by human trabecular meshwork cells. Invest Ophthalmol Vis Sci. 2004; 45(2):473–9. [PubMed: 14744887]

Cubey RB. Glaucoma following the application of corticosteroid to the skin of the eyelids. Br Journal Dermatol. 1976; 95(2):207–8.

Cukierman E, Pankov R, Stevens DR, Yamada KM. Taking cell-matrix adhesions to the third dimension. Science. 2001; 294(5547):1708–12. [PubMed: 11721053]

De Groef L, Van Hove I, Dekeyster E, Stalmans I, Moons L. MMPs in the trabecular meshwork: promising targets for future glaucoma therapies? Invest Ophthalmol Vis Sci. 2013; 54(12):7756–63. [PubMed: 24265206]

Fautsch MP, Bahler CK, Jewison DJ, Johnson DH. Recombinant TIGR/MYOC increases outflow resistance in the human anterior segment. Invest Ophthalmol Vis Sci. 2000; 41(13):4163–8. [PubMed: 11095610]

Fujimoto T, Inoue T, Kameda T, Kasaoka N, Inoue-Mochita M, Tsuboi N, Tanihara H. Involvement of RhoA/Rho-associated kinase signal transduction pathway in dexamethasone-induced alterations in aqueous outflow. Invest Ophthalmol Vis Sci. 2012; 53(11):7097–108. [PubMed: 22969074]

Gabelt, BT.; Kaufman, PL. Aqueous Humor Hydrodynamics. In: Hart, WM., editor. Adler's Physiology of the Eye. 9. St. Louis, MO: Mosby; 2003.

Garbe E, LeLorier J, Boivin JF, Suissa S. Inhaled and nasal glucocorticoids and the risks of ocular hypertension or open-angle glaucoma. JAMA. 1997; 277(9):722–7. [PubMed: 9042844]

Garrott HM, Walland MJ. Glaucoma from topical corticosteroids to the eyelids. Clin Exp Ophthalmol. 2004; 32(2):224–6.

Geiger B, Bershadsky A, Pankov R, Yamada KM. Transmembrane crosstalk between the extracellular matrix--cytoskeleton crosstalk. Nature reviews. Mol Cell Biol. 2001; 2(11):793–805.

Gerometta R, Spiga MG, Borras T, Candia OA. Treatment of sheep steroid-induced ocular hypertension with a glucocorticoid-inducible MMP1 gene therapy virus. Invest Ophthalmol Vis Sci. 2010; 51(6):3042–8. [PubMed: 20089869]

Giaever I, Keese CR. Monitoring fibroblast behavior in tissue culture with an applied electric field. Proc Nat Acad Sci U S A. 1984; 81(12):3761–4.

Gonzalez-Avila G, Ginebra M, Hayakawa T, Vadillo-Ortega F, Teran L, Selman M. Collagen metabolism in human aqueous humor from primary open-angle glaucoma. Decreased degradation and increased biosynthesis play a role in its pathogenesis. Arch Ophthalmol. 1995; 113(10):1319–23. [PubMed: 7575267]

Hoare MJ, Grierson I, Brotchie D, Pollock N, Cracknell K, Clark AF. Cross-linked actin networks (CLANs) in the trabecular meshwork of the normal and glaucomatous human eye in situ. Invest Ophthalmol Vis Sci. 2009; 50(3):1255–63. [PubMed: 18952927]

Honjo M, Tanihara H, Inatani M, Kido N, Sawamura T, Yue BY, Narumiya S, Honda Y. Effects of rho-associated protein kinase inhibitor Y-27632 on intraocular pressure and outflow facility. Invest Ophthalmol Vis Sci. 2001; 42(1):137–44. [PubMed: 11133858]

Johnson D, Gottanka J, Flugel C, Hoffmann F, Futa R, Lutjen-Drecoll E. Ultrastructural changes in the trabecular meshwork of human eyes treated with corticosteroids. Arch Ophthalmol. 1997; 115(3): 375–83. [PubMed: 9076211]

Johnson DH. The effect of cytochalasin D on outflow facility and the trabecular meshwork of the human eye in perfusion organ culture. Invest Ophthalmol Vis Sci. 1997; 38(13):2790–9. [PubMed: 9418732]

Johnson DH, Bradley JM, Acott TS. The effect of dexamethasone on glycosaminoglycans of human trabecular meshwork in perfusion organ culture. Invest Ophthalmol Vis Sci. 1990; 31(12):2568–71. [PubMed: 2125032]

Jones R 3rd, Rhee DJ. Corticosteroid-induced ocular hypertension and glaucoma: a brief review and update of the literature. Curr Opin Ophthalmol. 2006; 17(2):163–7. [PubMed: 16552251]

Kalina RE. Increased intraocular pressure following subconjunctival corticosteroid administration. Arch Ophthalmol. 1969; 81(6):788–90. [PubMed: 5783749]

Kersey JP, Broadway DC. Corticosteroid-induced glaucoma: a review of the literature. Eye. 2006; 20(4):407–16. [PubMed: 15877093]

Kopczynski CC, Epstein DL. Emerging trabecular outflow drugs. J Ocul Pharmacol Ther. 2014; 30(2-3):85–7. [PubMed: 24304197]

Lutjen-Drecoll E, May CA, Polansky JR, Johnson DH, Bloemendal H, Nguyen TD. Localization of the stress proteins alpha B-crystallin and trabecular meshwork inducible glucocorticoid response protein in normal and glaucomatous trabecular meshwork. Invest Ophthalmol Vis Sci. 1998; 39(3): 517–25. [PubMed: 9501861]

Matsumoto Y, Johnson DH. Dexamethasone decreases phagocytosis by human trabecular meshwork cells in situ. Invest Ophthalmol Vis Sci. 1997a; 38(9):1902–7. [PubMed: 9286282]

Matsumoto Y, Johnson DH. Trabecular meshwork phagocytosis in glaucomatous eyes. Ophthalmologica. 1997b; 211(3):147–52. [PubMed: 9176895]

Olson MW, Gervasi DC, Mobashery S, Fridman R. Kinetic analysis of the binding of human matrix metalloproteinase-2 and -9 to tissue inhibitor of metalloproteinase (TIMP)-1 and TIMP-2. J Biol Chem. 1997; 272(47):29975–83. [PubMed: 9368077]

Pang IH, Hellberg PE, Fleenor DL, Jacobson N, Clark AF. Expression of matrix metalloproteinases and their inhibitors in human trabecular meshwork cells. Invest Ophthalmol Vis Sci. 2003; 44(8): 3485–93. [PubMed: 12882798]

Provenzano PP, Inman DR, Eliceiri KW, Keely PJ. Matrix density-induced mechanoregulation of breast cell phenotype, signaling and gene expression through a FAK-ERK linkage. Oncogene. 2009; 28(49):4326–43. [PubMed: 19826415]

Quigley HA, Broman AT. The number of people with glaucoma worldwide in 2010 and 2020. Br J Ophthalmology. 2006; 90(3):262–7.

Rao PV, Deng PF, Kumar J, Epstein DL. Modulation of aqueous humor outflow facility by the Rho kinase-specific inhibitor Y-27632. Invest Ophthalmol Vis Sci. 2001; 42(5):1029–37. [PubMed: 11274082]

Read AT, Chan DW, Ethier CR. Actin structure in the outflow tract of normal and glaucomatous eyes. Exp Eye Res. 2007; 84(1):214–26. [PubMed: 17219625]

Sabanay I, Tian B, Gabelt BT, Geiger B, Kaufman PL. Functional and structural reversibility of H-7 effects on the conventional aqueous outflow pathway in monkeys. Exp Eye Res. 2004; 78(1):137–50. [PubMed: 14667835]

Samples JR, Alexander JP, Acott TS. Regulation of the levels of human trabecular matrix metalloproteinases and inhibitor by interleukin-1 and dexamethasone. Invest Ophthalmol Vis Sci. 1993; 34(12):3386–95. [PubMed: 8225873]

Sanka K, Maddala R, Epstein DL, Rao PV. Influence of actin cytoskeletal integrity on matrix metalloproteinase-2 activation in cultured human trabecular meshwork cells. Invest Ophthalmol Vis Sci. 2007; 48(5):2105–14. [PubMed: 17460268]

Snyder RW, Stamer WD, Kramer TR, Seftor RE. Corticosteroid treatment and trabecular meshwork proteases in cell and organ culture supernatants. Exp Eye Res. 1993; 57(4):461–8. [PubMed: 8282032]

Stolwijk JA, Matrougui K, Renken CW, Trebak M. Impedance analysis of GPCR-mediated changes in endothelial barrier function: overview and fundamental considerations for stable and reproducible measurements. Pflugers Archiv. 2015; 467(10):2193–218. [PubMed: 25537398]

Tanihara H, Inatani M, Honjo M, Tokushige H, Azuma J, Araie M. Intraocular pressure-lowering effects and safety of topical administration of a selective ROCK inhibitor, SNJ-1656, in healthy volunteers. Arch Ophthalmol. 2008; 126(3):309–15. [PubMed: 18332309]

Tanihara H, Inoue T, Yamamoto T, Kuwayama Y, Abe H, Araie M. Phase 2 randomized clinical study of a Rho kinase inhibitor, K-115, in primary open-angle glaucoma and ocular hypertension. Am J Ophthalmol. 2013; 156(4):731–6. [PubMed: 23831221]

Tian B, Kaufman PL. Effects of the Rho kinase inhibitor Y-27632 and the phosphatase inhibitor calyculin A on outflow facility in monkeys. Exp Eye Res. 2005; 80(2):215–25. [PubMed: 15670800]

Tokushige H, Inatani M, Nemoto S, Sakaki H, Katayama K, Uehata M, Tanihara H. Effects of topical administration of y-39983, a selective rho-associated protein kinase inhibitor, on ocular tissues in rabbits and monkeys. Invest Ophthalmol Vis Sci. 2007; 48(7):3216–22. [PubMed: 17591891]

Torrejon KY, Pu D, Bergkvist M, Danias J, Sharfstein ST, Xie Y. Recreating a human trabecular meshwork outflow system on microfabricated porous structures. Biotechnol Bioeng. 2013; 110(12):3205–18. [PubMed: 23775275]

Tripathi BJ, Tripathi RC, Chen J, Gotsis S, Li J. Trabecular cell expression of fibronectin and MMP-3 is modulated by aqueous humor growth factors. Exp Eye Res. 2004; 78(3):653–60. [PubMed: 15106945]

Tripathi BJ, Tripathi RC, Swift HH. Hydrocortisone-induced DNA endoreplication in human trabecular cells in vitro. Exp Eye Res. 1989; 49(2):259–70. [PubMed: 2767172]

Tripathi RC, Borisuth NS, Li J, Tripathi BJ. Growth factors in the aqueous humor and their clinical significance. J Glaucoma. 1994; 3(3):248–58. [PubMed: 19920605]

Tripathi, RC.; Tripathi, BJ. Functional anatomy of the anterior chamber angle. T, WW.; J, EA., editors. Philadelphia (PA): JB Lippincott Co; 1989.

Ueda J, Wentz-Hunter K, Yue BY. Distribution of myocilin and extracellular matrix components in the juxtacanalicular tissue of human eyes. Invest Ophthalmol Vis Sci. 2002; 43(4):1068–76. [PubMed: 11923248]

Vittitow J, Borras T. Genes expressed in the human trabecular meshwork during pressure-induced homeostatic response. J Cell Physiol. 2004; 201(1):126–37. [PubMed: 15281095]

Wen FQ, Kohyama T, Skold CM, Zhu YK, Liu X, Romberger DJ, Stoner J, Rennard SI. Glucocorticoids modulate TGF-beta production by human fetal lung fibroblasts. Inflammation. 2003; 27(1):9–19. [PubMed: 12772773]

Williams RD, Novack GD, van Haarlem T, Kopczynski C. Ocular hypotensive effect of the Rho kinase inhibitor AR-12286 in patients with glaucoma and ocular hypertension. Am J Ophthalmol. 2011; 152(5):834–41. e1. [PubMed: 21794845]

Wordinger RJ, Clark AF. Effects of glucocorticoids on the trabecular meshwork: towards a better understanding of glaucoma. Prog Retin Eye Res. 1999; 18(5):629–67. [PubMed: 10438153]

Yoneda A, Ushakov D, Multhaupt HA, Couchman JR. Fibronectin matrix assembly requires distinct contributions from Rho kinases I and -II. Mol Biol Cell. 2007; 18(1):66–75. [PubMed: 17065553]

Yue BY. The extracellular matrix and its modulation in the trabecular meshwork. Surv Ophthalmol. 1996; 40(5):379–90. [PubMed: 8779084]

Zhang X, Ognibene CM, Clark AF, Yorio T. Dexamethasone inhibition of trabecular meshwork cell phagocytosis and its modulation by glucocorticoid receptor beta. Exp Eye Res. 2007; 84(2):275–84. [PubMed: 17126833]

Zhong C, Chrzanowska-Wodnicka M, Brown J, Shaub A, Belkin AM, Burridge K. Rho-mediated contractility exposes a cryptic site in fibronectin and induces fibronectin matrix assembly. J Cell Biol. 1998; 141(2):539–51. [PubMed: 9548730]

Zhou L, Li Y, Yue BY. Glucocorticoid effects on extracellular matrix proteins and integrins in bovine trabecular meshwork cells in relation to glaucoma. Int J Mol Med. 1998; 1(2):339–46. [PubMed: 9852235]

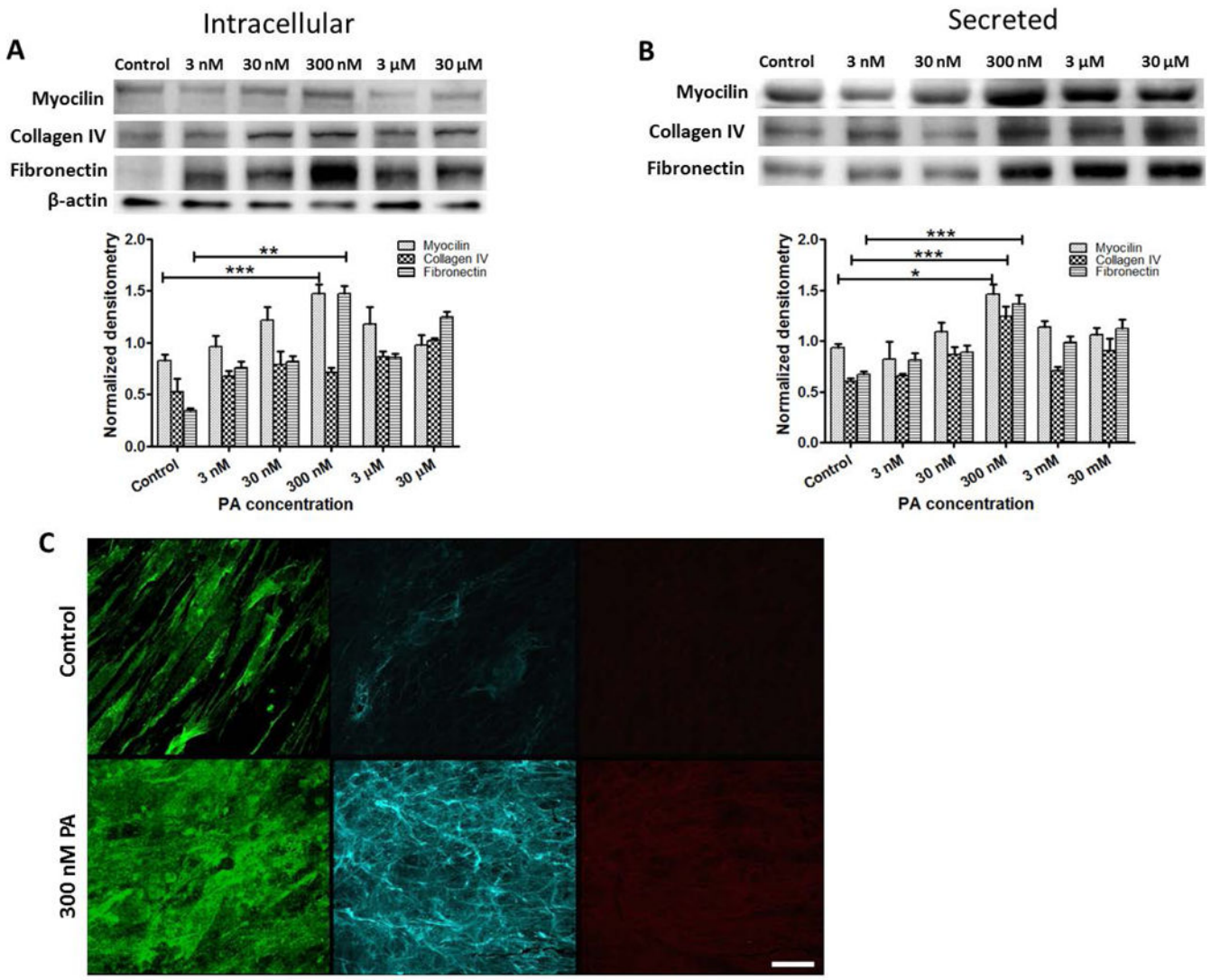

Figure 1.

Effects of glucocorticoid treatment on expression of myocilin and ECM proteins in 3D HTM cultures. Western blot analysis of dose-response to prednisolone acetate (PA) on (A) intracellular expression and (B) secretion of myocilin, collagen IV, and fibronectin. (C) Confocal images of immunocytochemistry of myocilin (left), collagen IV (middle) and fibronectin (right) in 3D HTM after perfusion with vehicle control (top panel) or 300 nM PA (lower panel) for 9 days. Scale bar = 40 µm.

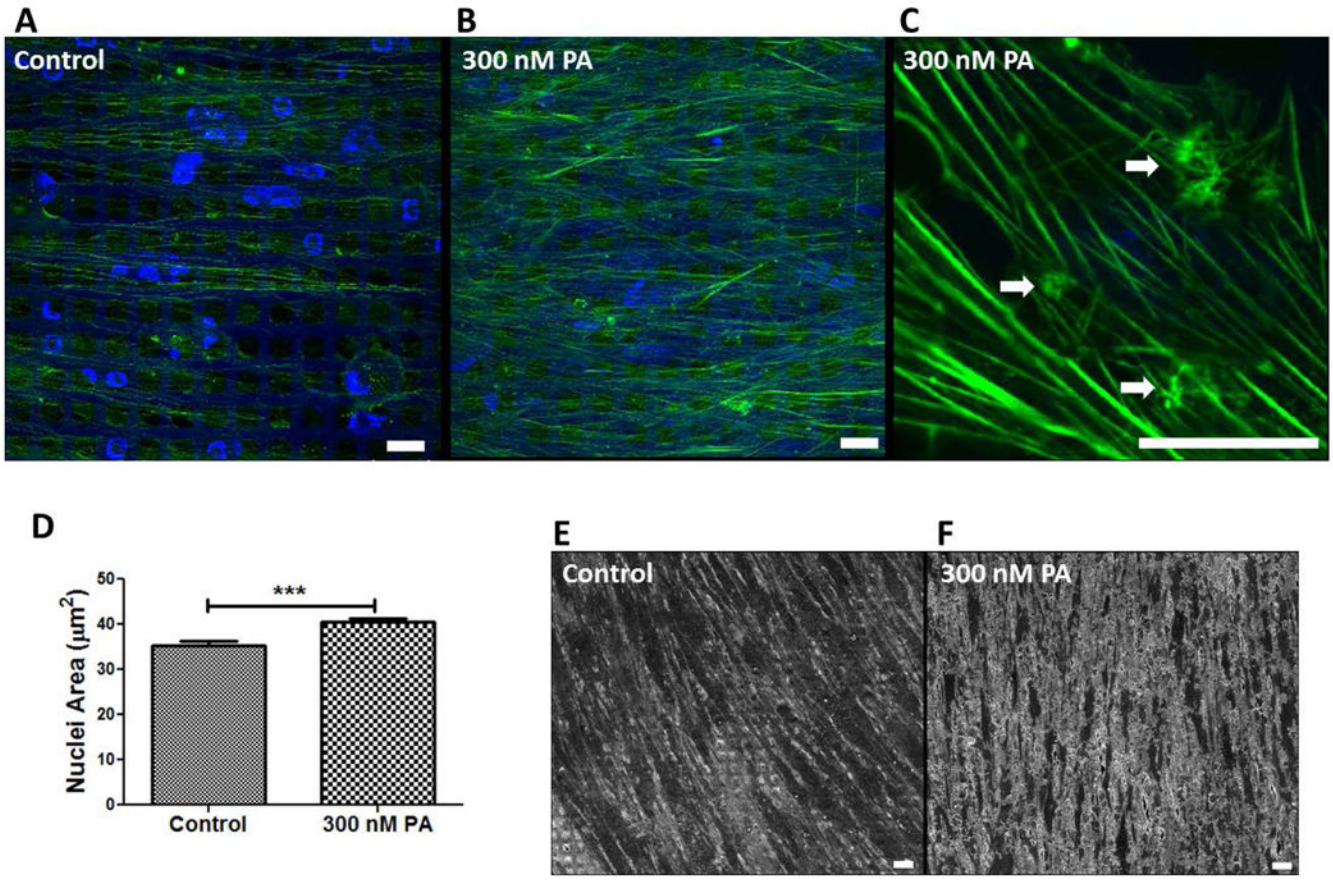

Figure 2.

Effects of glucocorticoid on actin cytoskeleton and nuclear size in 3D HTM. (A-C) Confocal images of phalloidin-stained F-actin in untreated control (A) and treated with 300 nM PA for 9 days (B and C). Arrow heads indicate CLANs. (D) Quantification of nuclear size after PA treatment compared to control. (E and F) SEM images of cell morphology in 3D HTM of control (E) or with PA-treatment (F). Scale bar = 20 μm.

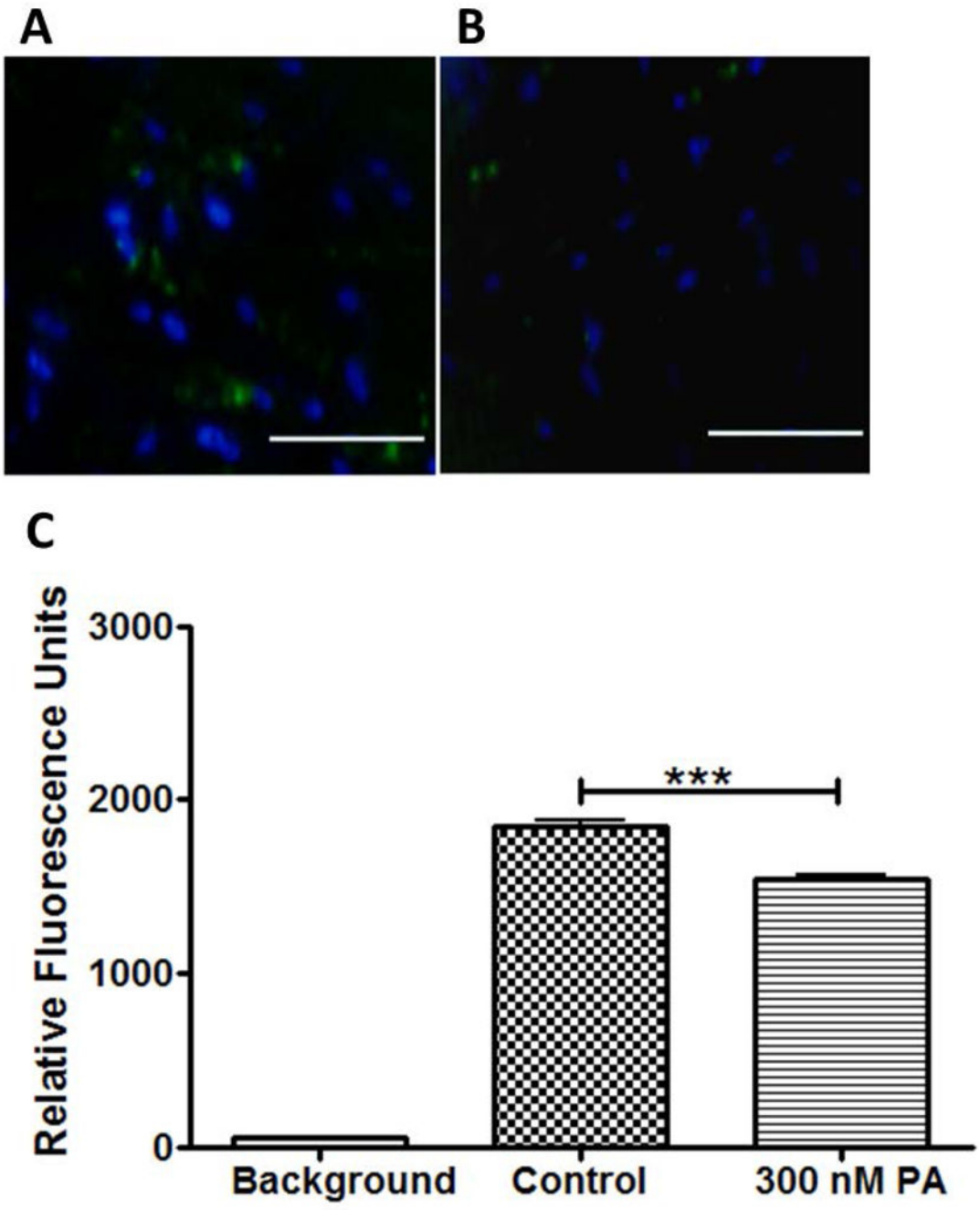

Figure 3.

Inhibition of phagocytic activity of 3D HTM cultures after treatment with glucocorticoid. Confocal images of phagocytic 3D HTM of control cultures (A) and cultures treated with 300 nM PA for 3 days (B). Scale bar = 200 μm. (C) Quantitation of fluorescence analysis of phagocytic activity.

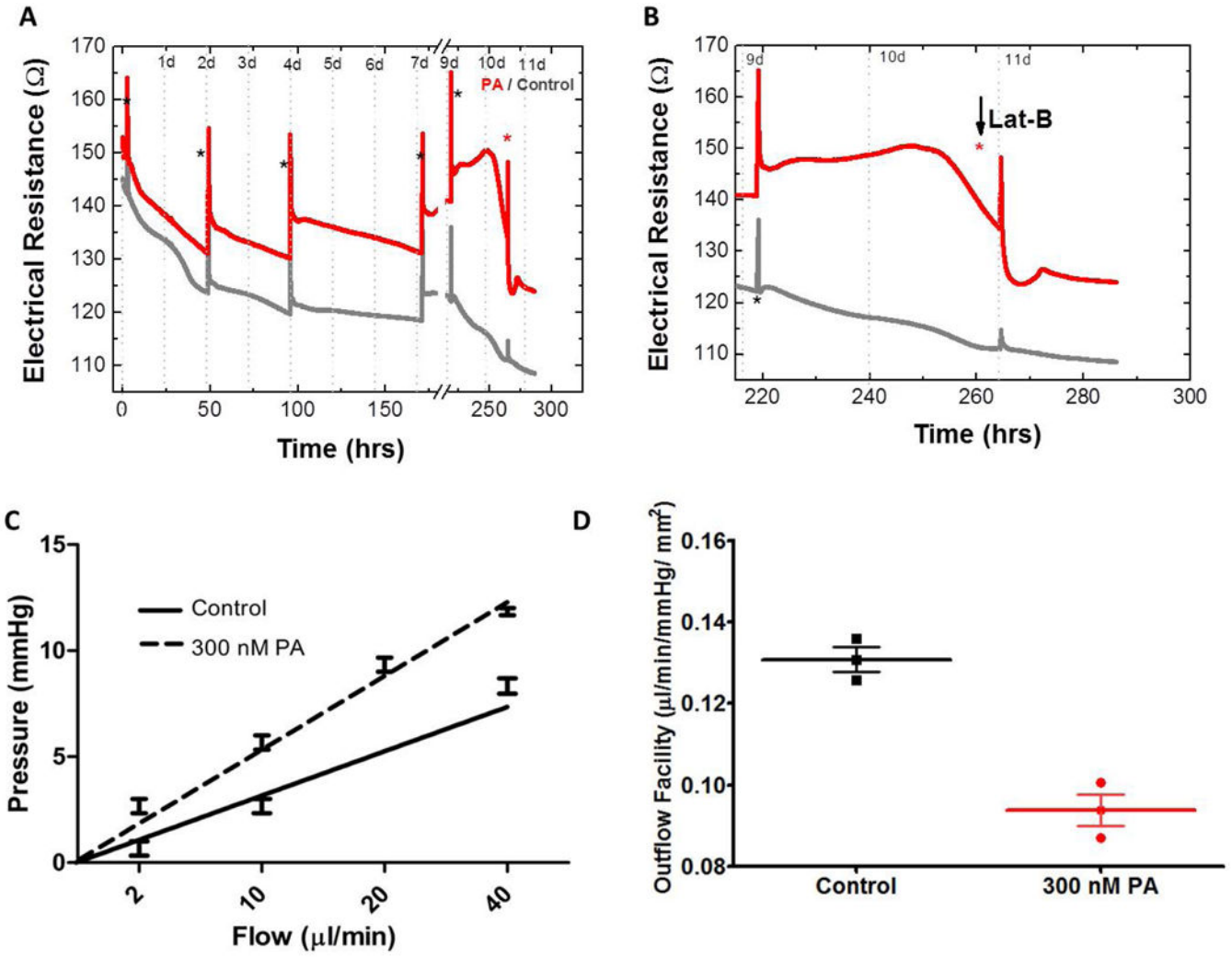

Figure 4.

Glucocorticoid-induced outflow resistance in 3D HTM. Electrical resistance during 11-day of PA-treatment with the addition of Lat-B (A) and enlarged graph for Lat-B treatment (B). Black asterisks indicate medium changes; red asterisk indicates addition of Lat-B. (C) Trans-scaffold pressure as a function of flow rate. (D) Outflow facility.

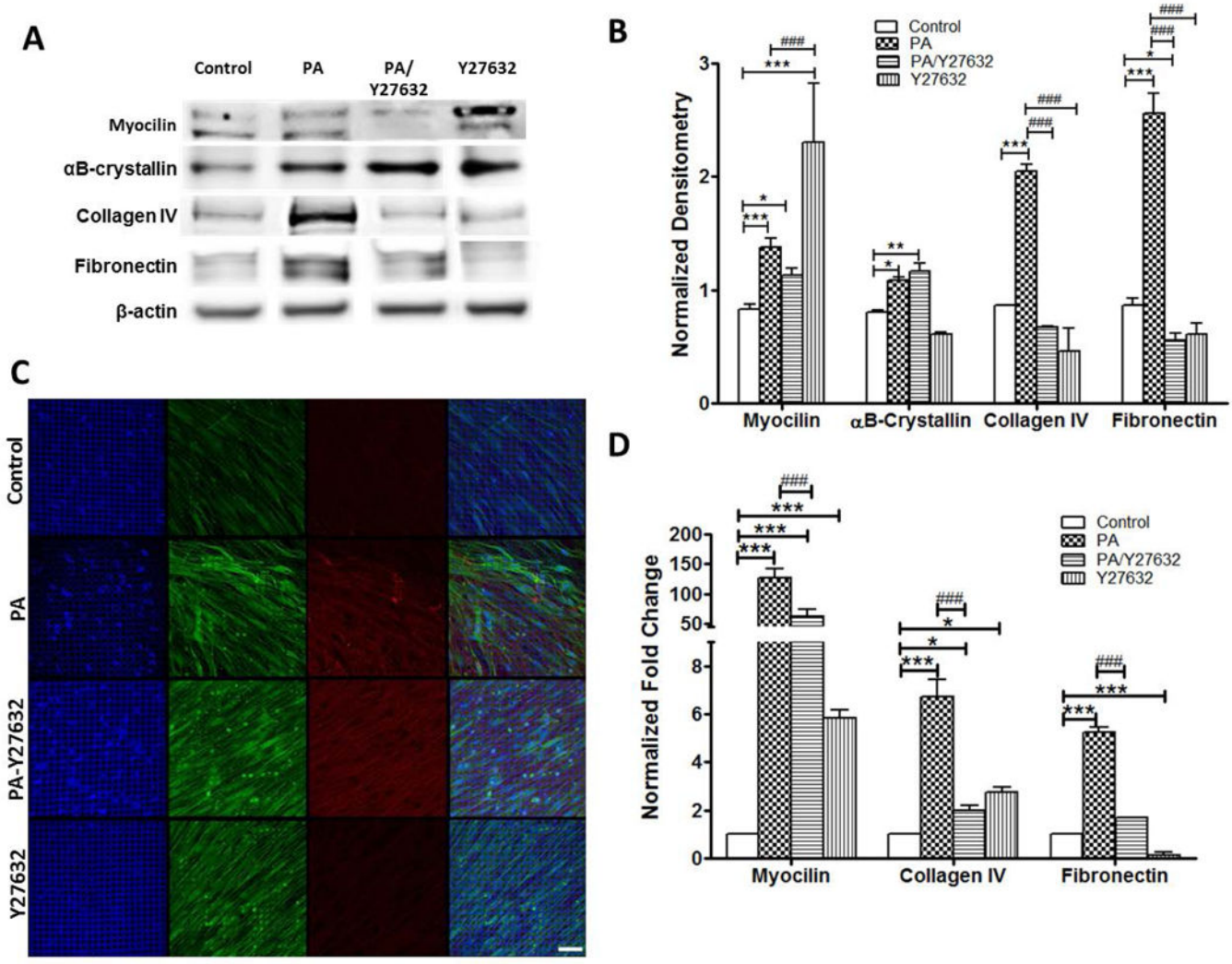

Figure 5.

Expression of trabecular meshwork markers and ECM proteins in 3D HTM treated with glucocorticoid and/or ROCK inhibitor (Y27632). (A) Western blot analysis of myocilin, αB-crystallin, fibronectin, and collagen IV for 3D-HTM scaffolds treated with ethanol (vehicle control), 300 nM PA, 300 nM PA + 10 μM Y27632 or 10 μM Y27632 alone for 9 days. (B) Densitometry analysis of western blot. * $P < 0.05$, ** $P < 0.005$, *** $P < 0.001$, $^{\#} P < 0.05$, $^{\#\#} P < 0.005$ and $^{\#\#\#} P < 0.001$. (C) Confocal images of myocilin and αB-crystallin expression in 3D-HTM after treatments. Blue: DAPI-stained nuclei. Green: myocilin. Red: αB-crystallin. Merged: right column. (D) qPCR analysis of gene expression of myocilin, collagen IV and fibronectin in 3D HTM after treatments.

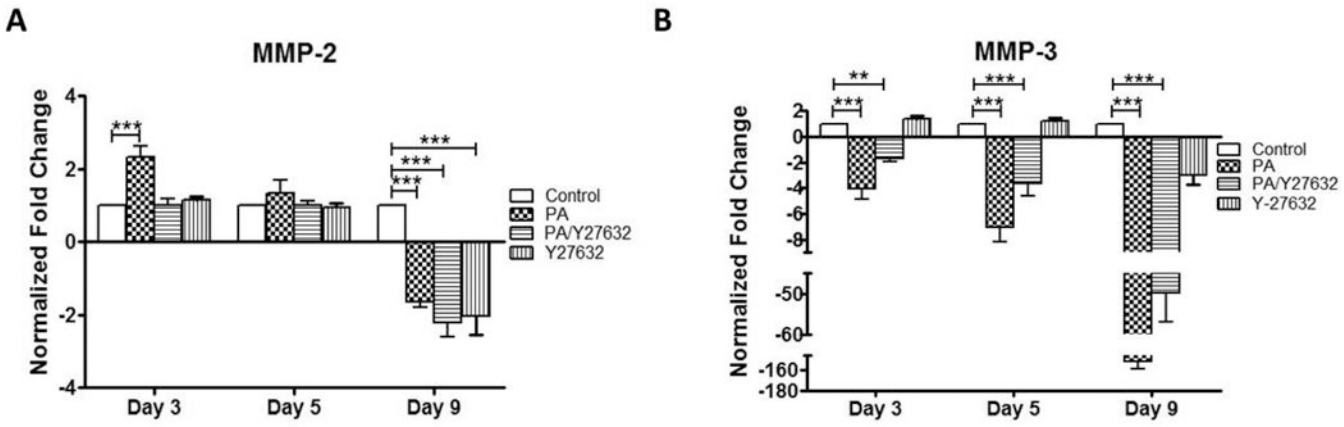

Figure 6.

qPCR analysis of MMP gene expression in 3D HTM after 3, 5 and 9 days of treatments with glucocorticoid (PA) and/or ROCK inhibitor (Y27632). (A) MMP-2. (B) MMP-3. * $P < 0.05$, ** $P < 0.005$ and *** $P < 0.001$.

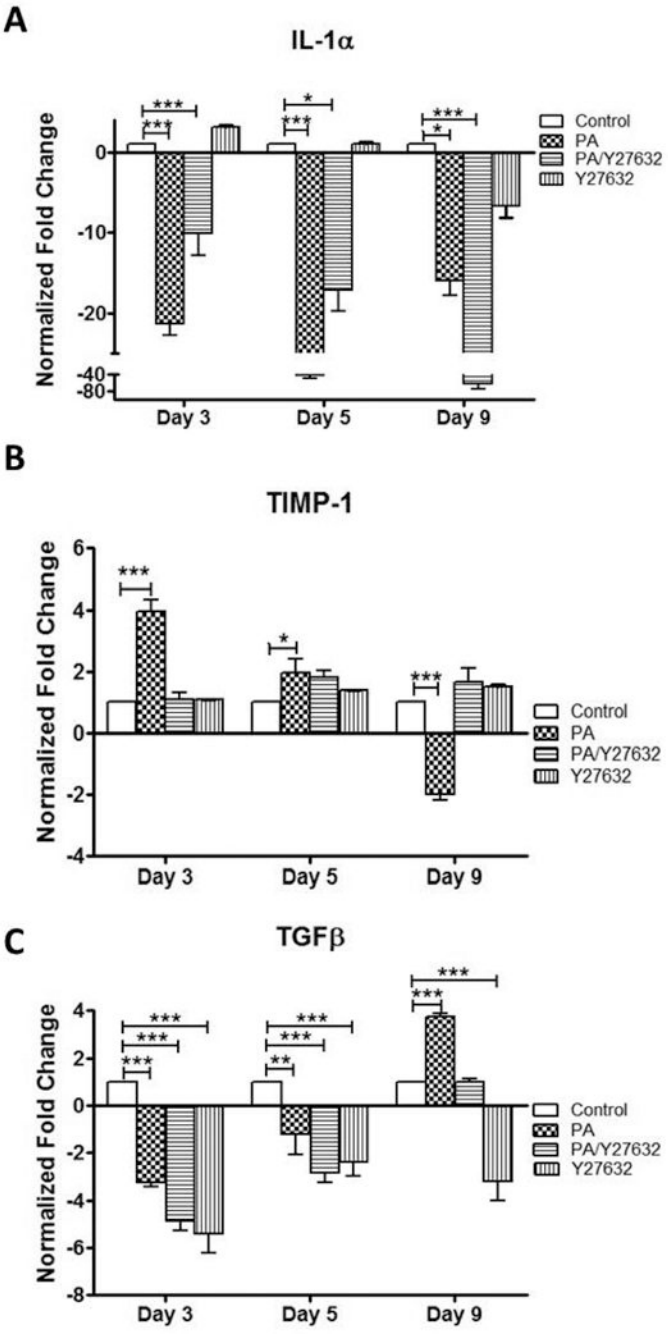

Figure 7.

qPCR analysis of gene expression of cytokines in 3D HTM after 3, 5 and 9 days of treatments with glucocorticoid (PA) and/or ROCK inhibitor (Y27632). (A) IL-1α. (B) TIMP-1. (C) TGFβ-2. * $P < 0.05$, ** $P < 0.005$ and *** $P < 0.001$.

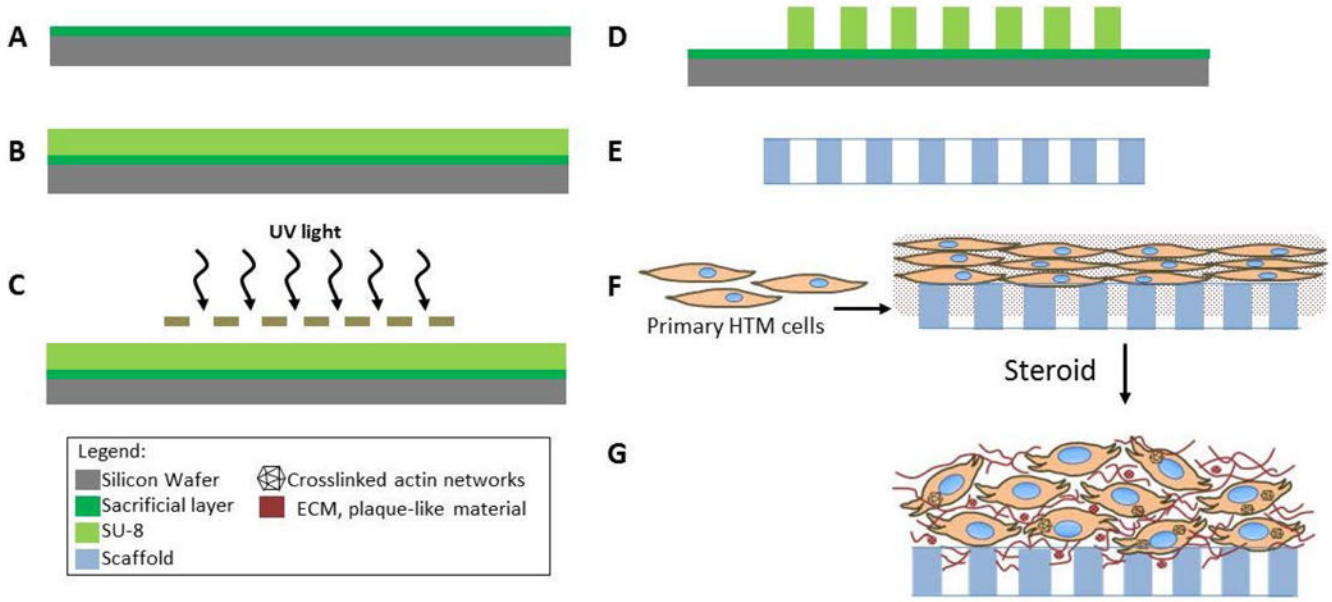

Scheme 1.

Creation of glaucomatous 3D HTM of microfabricated SU-8 scaffolds. (A) Pre-cleaned silica wafer treated with a sacrificial layer. (B) Photoresist SU-8 2010 coating. (C) UV-exposure using chrome mask. (D) post-exposure bake. (E) Development to produce SU-8 freestanding scaffold. (F) HTM cell seeding on the SU-8 scaffold followed by 3D culture. (G) Steroid-treatment to generate glaucomatous 3D HTM model.